# CRYSTALLIZATION: SIGNIFICANCE IN PRODUCT DEVELOPMENT, PROCESSING, AND PERFORMANCE

**Naír Rodríguez-Hornedo**
**Brent D. Sinclair**
*University of Michigan, Ann Arbor, Michigen, U.S.A.*

## INTRODUCTION

Understanding crystallization processes is important for the rational formulation, process development, and stability of pharmaceutical products. Whereas thermodynamics describes the equilibrium behavior of a system, pharmaceutical products most often encounter far-from-equilibrium conditions during processing, storage, or delivery. These conditions lead to the creation of metastable liquid or solid states. Metastable liquid states may include freeze concentrated solutions, solutions of weak acids or bases exposed to a pH change, solutions prepared by dissolution of salts of weak acids or bases, and solutions prepared by dissolution of a high energy form. Metastable solid states include amorphous solids, polymorphs, and solvates. Because crystallization provides a means to reduce the free energy of the system to the most stable state, crystallization mechanisms and kinetics determine the extent to which metastable states are reached and maintained.

Whereas knowledge of equilibrium phase diagrams is useful in identifying the concentration (or activity) and temperature regions of thermodynamic stability of solid phases, information on the crystallization kinetics is essential in determining solid phase outcomes. Nucleation and growth rates control the isolation of desired solid state modifications as well as the particle size distribution (number of particles, mean diameter, and standard deviation) and particle shape or morphology. The lack of information on crystallization processes leads to unwanted or previously unknown nucleation events that threaten the development of a pharmaceutical product. Dunitz and Bernstein (1) documented cases of "disappearing or elusive polymorphs," which provide evidence for the consequences of poor process control in crystallization of polymorphic systems. The recent shortage in the supply of capsules of the HIV protease inhibitor Norvir (ritonavir), due to the sudden formation of a crystalline structure different from the one harvested for months (2), illustrates the decisive role that nucleation mechanisms and kinetics have on crystallization. Nichols and Frampton (3) have reported considerable efforts that failed to crystallize the metastable polymorph of paracetamol as described in the initial publication of the crystal structure (4). The critical role of crystallization kinetics in determining the appearance of crystalline modifications is also recognized by the FDA and described in the guidelines for the manufacturing of drug substances (5): "Appropriate manufacturing and control procedures (including in-process testing when needed) should be established for the production of the desired solid-state form(s). It should be emphasized that the manufacturing process (or storage condition) is responsible for producing particular polymorphs or solvates; the control methods merely determine the outcome."

The goal of this chapter is to describe ways in which crystal structure, morphology, and crystallization kinetics can be utilized to reproducibly maintain metastable states and control solid-state outcomes. Experimental methods that can be employed to investigate the factors that regulate crystallization from solution will be presented.

## CRYSTALLIZATION

A crystalline phase is created as a consequence of molecular aggregation processes in solution. These prenucleation clusters may achieve a certain size for a sufficient time to enable growth into macroscopic crystals. The rate and mechanisms by which crystals form in liquid solutions are determined by numerous factors, including:

- Solubility or solubility product (solubility product is important in solutions of nonstoichiometric composition)
- Supersaturation: concentration of crystallizing solute or ions that participate in crystallization
- Diffusivity or viscosity
- Temperature
- pH
- Solvent
- Soluble additives and impurities
- Reactivity of surfaces toward nucleation
- Volume of solution

• Rate at which supersaturation is created: cooling rate, freezing rate, rate of pH change.

The effect of these factors on crystallization processes is thoroughly explained in various books (6–10).

Questions on the transferability of crystallization microtechniques to larger scale processes that are reproducible require careful consideration and study of crystallization kinetics. Whereas operationally useful variables that describe crystallization methods are often related to crystallization outcomes, this approach lacks meaningful information for developing a process that yields reliable outcomes because the factors that determine the crystallization kinetics and outcomes are not explicitly considered. For instance, compare the following two approaches to describe the processes for the selective crystallization of polymorphs: (1) form I obtained by cooling; form II obtained by evaporation; and (2) form I obtained at a supersaturation $x$, temperature $y$, and time $z$ at which crystals were harvested after crystallization onset; form II obtained at supersaturation $x'$, etc. Whereas the former approach is at best anecdotal, the latter employs the causative factors and leads to relationships between the crystallization kinetic parameters and the outcomes.

Control of the processes of nucleation and crystal growth is possible as long as the required information is available. In a study of crystallization of polymorphs of paracetamol by Nichols and Frampton (3), seeding with crystals of the desired solid phase and the time of harvesting the solid phase were found to have a significant effect on the isolation of the desired polymorph. The orthorhombic polymorph (metastable) could not be obtained by a previously reported method (4) "—slow evaporation from ethanol." Dunitz and Bernstein (1) have explained the mystery of disappearing polymorphs by considering various examples and the relevant questions that were left unanswered. They state that, "Once a particular polymorph has been obtained, it is always possible to obtain it again; it is only a matter of finding the right experimental conditions."

## SUPERSATURATION

A solid phase is precipitated from solution if the chemical potential of the solid phase is less than that of the dissolved component. A solution in which the chemical potential of the solute is the same as that of the corresponding solid phase is in equilibrium with the solid phase under the given conditions (temperature, pH, and concentration) and called a saturated solution. In order for crystallization to occur, however, this equilibrium concentration or solubility must be exceeded. This excess concentration or chemical potential is called supersaturation. Supersaturated states may be created by:

1. Methods that regulate the solute activity or activity product (concentration) include:
   a. solvent removal (evaporation or freezing);
   b. addition of indifferent salts with ions that participate in precipitation (addition of NaCl to sodium phosphate solution causing the precipitation of $Na_2HPO_4$); and
   c. dissolution of a metastable solid phase (transformations of amorphous to crystalline, anhydrous to hydrate, more soluble to less soluble polymorph, and salt to free acid or free base).
2. Methods that regulate the solute solubility include:
   a. temperature change;
   b. pH change; and
   c. addition of solvent or additives that lower the solubility of the solute.

Knowledge of the driving force for crystallization is essential, not only to characterize the kinetics but also to relate the crystallization outcomes to the parameters that regulate crystallization. The number of molecules required to achieve an effective nucleating cluster is inversely proportional to the supersaturation. Therefore, as the supersaturation is increased the probability of nucleation increases. However, nucleation is energetically more demanding than crystal growth, and there are supersaturation regions in which crystal growth proceeds while spontaneous nucleation is suppressed (metastable zone; 6,7,9).

The driving force for nucleation and growth is the difference in chemical potential of the solute in a supersaturated solution, $\mu_1$, and in a saturated solution, $\mu_{eq}$,:

$$\Delta\mu = (\mu_1 - \mu_{eq}) \tag{1}$$

Because $\mu = \mu^\circ + \mathrm{RT} \ln a$, then

$$\Delta\mu = \mathrm{RT}\ ln\ (a/a_{eq}) = \mathrm{RT} \ln (\gamma_1 c_1/\gamma_{eq} c_{eq}) \tag{2}$$

and the supersaturation is

$$\sigma = \Delta\mu/\mathrm{RT} = \ln (a/a_{eq}) = \ln (\gamma_1 c_1/\gamma_{eq} c_{eq}) \tag{3}$$

If the activity coefficient, $\gamma$, is independent of concentration in the given concentration regime, then $\gamma_1 = \gamma_{eq}$, and the supersaturation becomes

$$\sigma = \ln (c/c_{eq}) = \ln (c/s) \tag{4}$$

where c is the concentration of the crystallizing substance in the supersaturated solution and s is the solubility. (This

notation is adopted to avoid the use of subscripts.) For *c*/*s* values smaller than 1.15

$$\sigma = \ln (c/s) \approx (c - s)/s. \quad (5)$$

Frequently used expressions for supersaturation are [(c−s)/s] and the ratio (c/s). If the supersaturation is attained by changing the pH, then the ratio of the concentration of the solution to the solubility at the given pH is the supersaturation ratio. Fig. 1 illustrates an example of the effect that changing the pH can have on the supersaturation of a weakly basic drug ($pK_a = 5.25$). When the pH of the solution is increased along the path represented by line ABC, spontaneous crystallization will occur when the pH corresponding to point C is achieved. When this boundary is exceeded (i.e., pH increased past point C), the rate of nucleation rapidly increases and the crystallization process may become less controlled. The concentration in the solution decreases as nuclei form and grow until the equilibrium concentration at the final pH is reached at point D. If the concentration is maintained at a pH somewhere in between points B and C, the solution is in the metastable region—where the probability of spontaneous nucleation is negligible while crystal growth on seeds occurs.

## NUCLEATION

Nucleation is often the decisive step in the crystallization process and is of practical importance in pharmaceutical systems. Crystallization may occur intentionally or unintentionally during pharmaceutical processes in which supersaturated conditions are achieved. Pharmaceutical processes in which supersaturated states are attained due to solvent removal include: freezing, freeze drying, spray drying, and drying of wet granulations. Other processes achieve supersaturation by changing solubility, during isolation of solid state forms, or during dissolution of weak bases in an environment in which pH is changing, such as in the gastrointestinal tract, as previously described.

The concentration threshold at which crystallization is observed at times shorter than the processing time or desired product shelf-life or GI transit time, is determined by the kinetic stability of supersaturated states and is regulated by the nucleation mechanisms and kinetics. Nucleation phenomena are equally important in the control of micromeritic properties and in the selective crystallization of a particular polymorph.

The crystallization-induced pH changes that occur during the freezing of sodium phosphate buffers illustrate the importance of kinetic events in determining final pH and product stability. The pH changes of sodium phosphate buffers during freezing at close-to-equilibrium conditions have been thoroughly studied (11, 12), and the phase diagram—phases, composition, and pH—of sodium phosphate buffers during freezing is shown in Fig. 2. However, it is recognized that during freeze-drying, freezing does not take place close-to-equilibrium and that large undercoolings and supersaturations are often encountered (13–16). During cooling of hypoeutectic solutions of monosodium and disodium phosphate, ice crystallization increases the total salt concentration, and the ratio of the dissolved salts will change when precipitation of

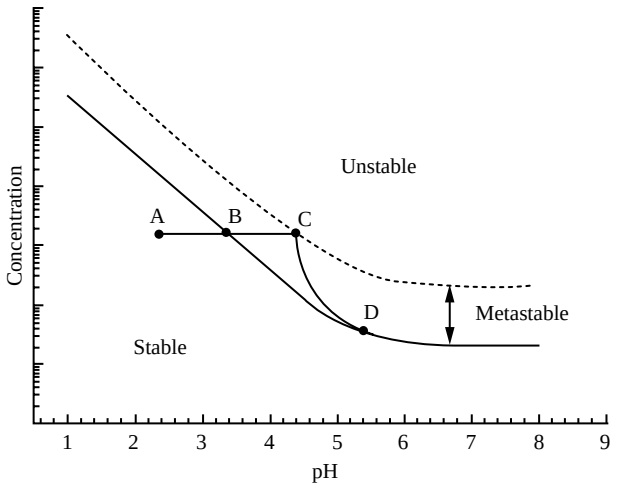


**Fig. 1** Regions of varying thermodynamic stability for solutions of a weak base as a function of pH.

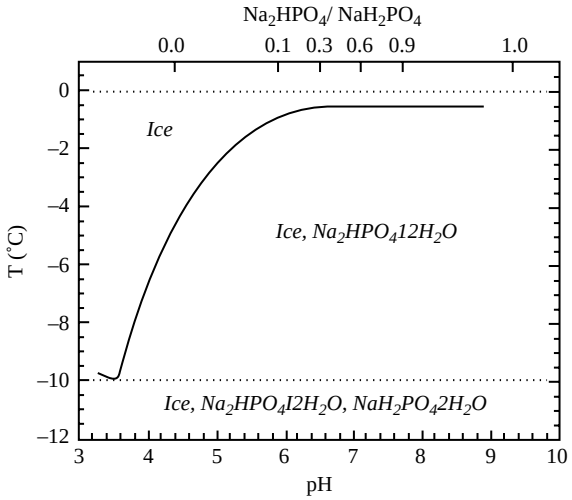


**Fig. 2** pH and ratio of mono- to disodium phosphate salts during equilibrium freezing of sodium phosphate buffers, at initial buffer concentration of 20 m*M*. (Based on Ref. 11.)

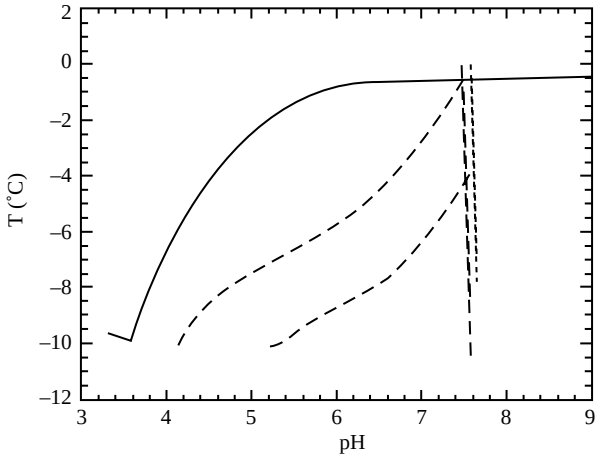


**Fig. 3** Comparison of pH during equilibrium and far–from–equilibrium freezing of sodium phosphate buffers. Equilibrium freezing, initial buffer concentration 20 m*M*, (—). Far–from–equilibrium freezing: Initial buffer concentrations of 100 mM (– – – –) and 8 mM (- - - -). (From Refs. 11 and 17).

one of the salts occurs. Disodium phosphate dodecahydrate is the least soluble salt in this system (eutectic temperature = −0.5°C and eutectic concentration = 0.11 *M*). Under close-to-equilibrium freezing, it precipitates first at initial pH values greater than 3.6, and at temperatures above the ternary eutectic of −9.9°C. This corresponds with the ternary eutectic composition at monosodium to disodium phosphate molar ratios of 3.42:0.06. Because precipitation of $Na_2HPO_4{\cdot}12H_2O$ consumes $HPO_4^{2-}$ ions, the pH of the unfrozen solution decreases to the equilibrium value of 3.6.

If one wishes to design a formulation to be freeze-dried in which the active product ingredient has a narrow pH range for optimal stability, at what initial pH and buffer concentration should the formulation be prepared before freezing so that the pH remains within the specified range during freezing? In other words, does selective salt crystallization occur at the freeze concentrations achieved during the freeze-drying process, and what is the concentration dependence of salt crystallization in such systems? Based on thermodynamic considerations, sodium phosphate buffer solutions are expected to reach a buffer concentration of 3.5 *M* and a pH of 3.6 upon freezing to −10°C, if crystallization of ice and $Na_2HPO_4{\cdot}12H_2O$ proceed to equilibrium. This may be the case in seeded systems under slow cooling rates in which the pH and composition of the residual solution follow very closely the phase diagram (Fig. 3) (11). In contrast to the equilibrium behavior, studies during far-from-equilibrium freezing of sodium phosphate buffers show that the more dilute buffer solutions (lower concentrations of precipitating ions) experience greater departures from equilibrium and maintain pH values as high as 3 units above the equilibrium pH values (17). Thus, crystallization-induced pH changes are determined by the factors that regulate salt crystallization kinetics and depend on the initial salt concentration (pH and concentration).

Whereas buffer salt concentrations are not directly measured during freezing, they can be calculated from in situ pH measurements. Temperature–pH time profiles during freezing reveal the onset of ice crystallization

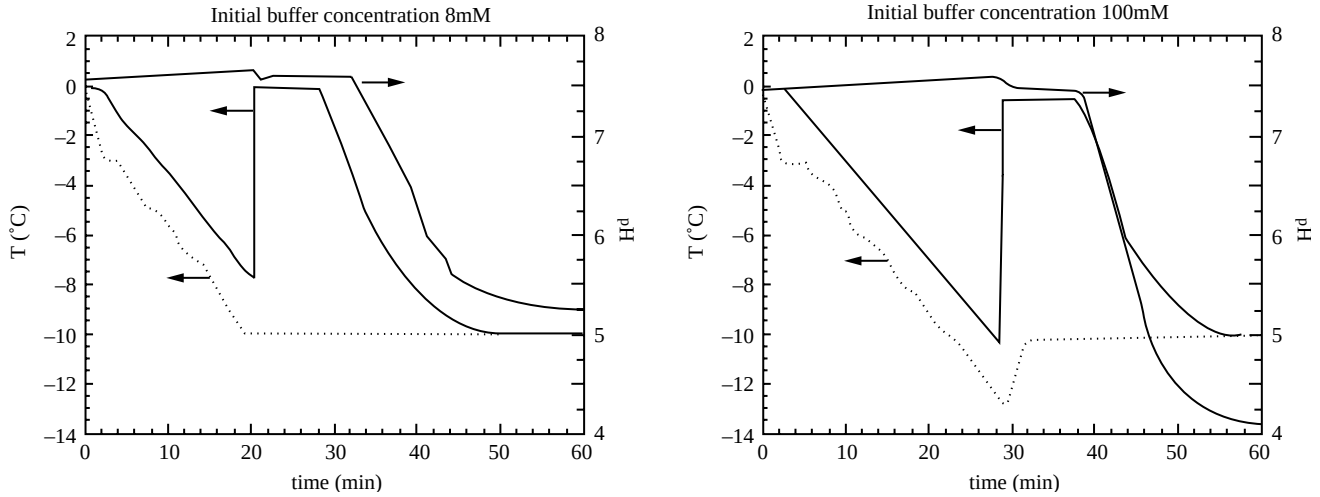


**Fig. 4** Effect of initial buffer concentration on pH during far–from–equilibrium freezing of sodium phosphate buffer solutions. Initial pH of 7.4 at 25°C and initial buffer concentration of 100 m*M* and 8 m*M*. Solution temperature (—), bath temperature (- - - -), and (—) pH. (From Ref. 17.)

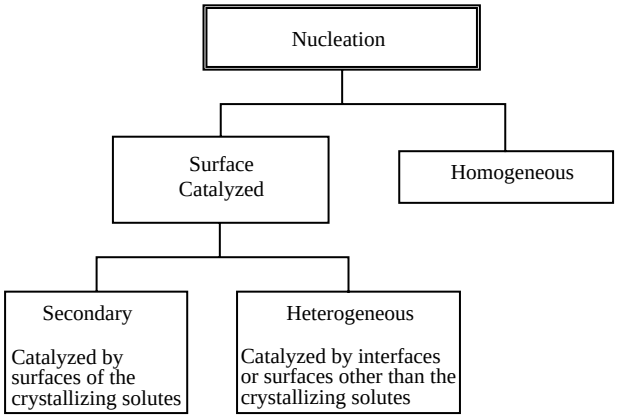


**Fig. 5** Mechanisms for crystal nucleation.

(increase in temperature) followed by $Na_2HPO_4 \cdot 12H_2O$ crystallization (decrease in pH) in sodium phosphate buffer solutions of initial pH 7.4 and initial concentration in the range of 8–100 m*M* (Fig. 4) (17). This salt precipitates very early in the freezing process and within 15 min. after the onset of ice crystallization.

## Nucleation Mechanisms

Nucleation mechanisms can be divided into two main categories: homogeneous and surface- or interface-catalyzed (7–9,18), as shown in Fig. 5. Homogeneous nucleation rarely occurs in large volumes (greater than 100 $\mu$l) because solutions contain random impurities that may induce nucleation (19, 20). This type of nucleation is referred to as heterogeneous. A surface or an interface of different composition than the crystallizing solute may serve as a nucleation substrate by decreasing the energy barrier for the formation of a nuclei that can grow into a mature crystal. Nucleation that is promoted by crystals of the crystallizing solute is known as secondary nucleation. These mechanisms are thoroughly discussed by Mullin (7), Myerson (9), and Zettlemoyer (18).

## Homogeneous Nucleation

Thermodynamic considerations for nucleation are based on the work of Gibbs (21), Volmer (22), and others, where the free energy change for an aggregate undergoing a phase transition $\Delta G$ is given by

$$\Delta G = \Delta G_V + \Delta G_S \tag{6}$$

where $\Delta G_s$ is the surface free energy change associated with the formation of the aggregate (a positive quantity), and $\Delta G_v$ is the volume free energy change associated with the phase transition (a negative quantity). For homogeneous or heterogeneous nucleation

$$\Delta G_V = -\alpha l^3 \upsilon k_B T \ln\left(\frac{c}{s}\right) \tag{7}$$

where $\alpha$ is the volume-shape factor, $l$ is the characteristic length, $\upsilon$ is the molecular volume of the crystallizing solute, $k_B$ is Boltzmann's constant, and $T$ is temperature. For homogeneous nucleation

$$\Delta G_s = \beta l^2 \gamma_{12}, \tag{8}$$

where $\beta$ is the area shape factor and $\gamma$ is the interfacial energy per unit area between the crystallization medium, 1, and the nucleating cluster, 2. Consequently, the overall free energy change for nucleation is decreased by a large supersaturation ratio ($c/s$) and by a low interfacial energy.

The factors that regulate nucleation are best appreciated by considering the equation for the rate of homogeneous nucleation from solutions:

$$\begin{aligned} J &= N_o \nu \exp\left(\frac{-\Delta G^*}{k_B T}\right) \\ &= N_o \nu \exp\left(\frac{-4\beta^3 \upsilon^2 \gamma_{12}^3}{27\alpha^2 (k_B T)^3 (\ln(cs))^2}\right) \end{aligned} \tag{9}$$

$J$ is the number of nuclei formed per unit time per unit volume, $N_o$ is the number of molecules of the crystallizing phase in a unit volume, $\nu$ is the frequency of atomic or molecular transport at the nucleus–liquid interface, and $\Delta G^*$ is the maximum in the Gibbs free energy change for the formation of clusters at a certain critical size, $l^*$. The nucleation rate was initially derived for condensation in vapors (23), where the pre-exponential factor is related to the gas kinetic collision frequency. In the case of nucleation from condensed phases, the frequency factor is related to the diffusion process (24). The value of $l^*$ can be obtained by minimizing the free energy function with respect to the characteristic length:

$$l^* = \frac{2\beta \upsilon \gamma_{12}}{3\alpha k_B T \ln\left(\frac{c}{s}\right)} \tag{10}$$

For spherical clusters, $\alpha = 4\pi/3$ and $\beta = 4\pi$, based on the radius of the cluster.Therefore,

$$r^* = \frac{2\upsilon \gamma_{12}}{k_B T \ln\left(\frac{c}{s}\right)} \tag{11}$$

Considering these geometric factors, the rate for homogeneous nucleation of spherical clusters is

$$J = N_o \nu \exp\left(\frac{-16\pi \upsilon^2 \gamma_1^3 2}{3(k_B T)^3 \left(\ln\left(\frac{C}{S}\right)\right)^2}\right) \quad (12)$$

Whereas the classical theory of nucleation is limited by the implicit assumptions in its derivation (described in detail in Ref. 6), it successfully predicts the nucleation behavior of a system (7–9, 18, 25). Inspection of the aforementioned equation clearly suggests that the nucleation rate can be experimentally controlled by the following parameters: molecular or ionic transport, viscosity, supersaturation, solubility, solid–liquid interfacial tension, and temperature.

Nucleation kinetics are experimentally determined from measurements of nucleation rates, induction times, and metastability zone widths (the supersaturation or undercooling necessary for spontaneous nucleation) as a function of initial supersaturation (6–8, 26). The nucleation rate will increase by increasing the supersaturation while all other variables are constant. However, at constant supersaturation, the nucleation rate will increase with increasing solubility. Solubility affects the pre-exponential factor and the probability of intermolecular collisions. Furthermore, when changes in solvent or solution composition lead to increases in solubility, the interfacial energy decreases because the affinity between crystallizing medium and crystal increases (6). Consequently, the supersaturation required for spontaneous nucleation decreases with increasing solubility (27), as shown in Fig. 6.

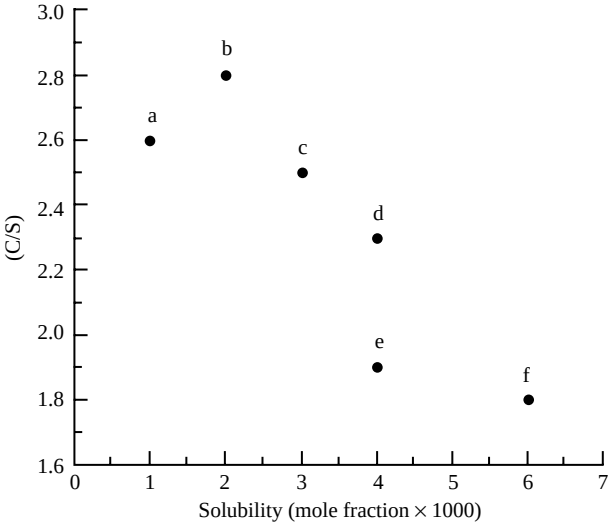


**Fig. 6** Dependence of the critical supersaturation for nucleation on solubility of nitrofurantoin in (a) formic acid, (b) formic acid: water (4:1), (c) formic acid: ethanol (2:1), (d) formic acid: dioxane (2:1), (e) formic acid: methanol (2:1), (f) formic acid: water (2:1). (From Ref. 27.)

The dependence of nucleation rate on solubility is also consistent with Ostwald's law of stages (28) regarding the preferential formation of a metastable solid phase. It states the following: "When leaving an unstable state, a system does not seek out the most stable state, rather the nearest metastable state which can be reached with loss of free energy." This indicates that if the unstable solid state modification (the system with highest solubility) precipitates before more thermodinamically stable solid phases, it must have higher nucleation and growth rates than solid states of lower solubility. However, Ostwald's law of stages is not universally valid because the appearance and evolution of solid phases are determined by the kinetics of nucleation and growth under the specific experimental conditions (29–31).

Accounts of nucleation inhibition in the pharmaceutical literature are sometimes confusing because the dependence of the nucleation event (nucleation rate, metastability zone width, or induction time) on supersaturation is not considered. In search of additives that inhibit nucleation, induction times are often measured as a function of additive concentration, whereas the dependence of the nucleation event on supersaturation is neglected. Results from such studies possibly lead to the erroneous conclusion that the additive inhibited nucleation (32, 33) when, indeed, the additive decreased the supersaturation and frequently led to an undersaturated state. Hence, the system is under thermodynamic control instead of kinetic control.

An important factor contributing to the nucleation mechanism and kinetics is the volume of solution in which nucleation occurs. The dispersal of a bulk liquid into a collection of small droplets has been shown to be an effective way of achieving large supersaturations or undercoolings (19, 20). Precipitation and solidification in small volumes (droplets) involving emulsions have been used to study homogeneous nucleation processes (34) and for the control of purity, particle size, and morphology (35, 36). Dispersing a solution into small volumes isolates heterogeneous nucleants within a fraction of the drops and makes nucleation more difficult. Consequently, larger supersaturations need to be reached for nucleation to occur. The boundaries of possible outcomes are represented by the following scenarios: (1) crystals of very small size (even in the nanometer range) are formed as a result of the high nucleation rates (35, 36), or (2) a glass or amorphous solid is formed due to the low diffusion rates of molecules that inhibit the evolution of clusters to crystals within the time scale of the experiment (37).

Nucleation outcomes from solutions with initially the same composition may vary as a consequence of impurities, rates at which supersaturation was created, thermal histories, experimental techniques employed to detect

**Table 1** Disodium phosphate crystallization behavior during far-from-equilibrium freezing of buffer solutions

| Observation | $C_{Na_2HPO_4}$[a] (m*M*) | Reference |
|---|---|---|
| Crystallization begins to decrease | ≤200 | Murase and Franks (16, 38) |
| Does not crystallize | ≤10 | |
| Crystallization begins to decrease | ≤15 | Gómez (17) |
| Crystallization readily occurs | ≥0.3 | |
| Crystallization is not inhibited by $C_{NaH_2PO_4}$[b] ≤ 94 m*M* | 6 | |
| Readily crystallizes | 190 | Cavatur and |
| Crystallization inhibited by $C_{NaH_2PO_4}$ ≥ 730 m*M* | 190 | Suryanarayanan (39) |

[a] $C_{Na_2HPO_4}$ = initial disodium phosphate concentration in solution at 25°C.
[b] $C_{NaH_2PO_4}$ = initial monosodium phosphate concentration in solution at 25°C.

precipitation, and solution volumes in which nucleation occurred. This is illustrated by comparing results of the selective crystallization of buffer components during freezing from various laboratories (16, 17, 38–39). The initial salt concentrations and the crystallization behavior of disodium phosphate during freezing of sodium phosphate buffer solutions are shown in Table 1. Murase et al. (16, 38) report that disodium phosphate precipitation occurs at higher initial buffer and disodium phosphate concentrations, compared to those observed in our laboratory (17). Murase et al. report that salt precipitation begins to decrease at initial buffer concentrations below 500 m*M*, corresponding to 200 m*M* disodium phosphate, compared with results from our studies where decreases in salt precipitation were detected at initial buffer concentrations below 8 m*M*, corresponding to 0.3 m*M* disodium phosphate. Furthermore, disodium phosphate did not precipitate at initial disodium salt concentrations below 10 m*M*, whereas our studies show that precipitation occurs at salt concentrations as low as 0.3 m*M*. Inspection of the experimental conditions under which these studies were done (Table 2) shows a trend towards lower extent of crystallization (and slower crystallization rates) with decreasing volume of solutions from 25 ml to 3 μl and increasing rates of cooling to lower temperatures.

Neglecting the factors that regulate nucleation leads to misleading generalizations when developing guidelines to control precipitation by the addition of noncrystallizing additives. Consider, for example, the conflicting interpretation of additive effects on nucleation when these are expressed in terms of concentration ratios (additive to crystallizing solute) while ignoring other parameters. Data in Table 1 indicates that disodium phosphate precipitation is inhibited at ($H_2PO_4^-/HPO_4^{2-}$) ≤ 4 (0.73 *M* 0.19 *M*) (39) whereas it is not inhibited at $H_2PO_4^-/HPO_4^{2-}$) ≥ 16 (0.094 M/0.006M) (17). Compared to the systems we studied, the buffers studied by Cavatur and Suryanarayanan (39) have much higher concentrations of monosodium phosphate (which increases the viscosity of solutions) in addition to smaller solution volumes and faster rates of cooling to lower temperatures. All of these factors contribute to delaying precipitation.

The effect of the viscosity of the crystallization medium on the nucleation rate has been described by Turnbull and Fisher (24). The frequency of atomic or molecular transport at the nucleus-liquid interface, $\nu$, can be related to the bulk viscosity, $\eta$, with the Stokes–Einstein relation:

$$\nu \approx \frac{kT}{3\pi a_o^3 \eta(T)} \tag{13}$$

**Table 2** Experimental conditions and methods of measuring progress of sodium phosphate crystallization during freezing

| Reference | Volume of solution (μl) | Cooling rate (°C/min) | Temperature (°C) | Method |
|---|---|---|---|---|
| Murase and Franks (16, 38) | 2–5 | 0.62 | −52 | DSC, SEM |
| Gómez (17) | $25 \times 10^3$ | 0.3–0.5 | −10 | pH |
| Cavatur and Suryanarayanan (39) | 300[a] | 15 | −40 | XRPD |

[a] Personal communication.

where $a_o$ is the mean effective diameter of the diffusing species. If the viscosity dependence on temperature is described by Arrhenius behavior, then

$$J = \frac{K}{\eta_o}\exp\left(\frac{-\Delta G^* - \Delta G_a}{kT}\right) \quad (14)$$

where $\Delta G_a$ is the activation energy for transport across the nucleus–liquid interface. Thus, the nucleation rate may go through a maximum when an increase in undercooling or supersaturation is accompanied by an increase in viscosity. This behavior has been observed in the nucleation of citric acid in aqueous solutions (40) and the crystallization of ice (41).

## Heterogeneous Nucleation

Heterogeneous nucleation processes are of fundamental and practical importance in pharmaceutical systems because unintentionally or intentionally added surfaces or interfaces may promote nucleation. The reactivity of crystal surfaces as heterogeneous nucleants has significant consequences in the isolation of the desired solid-state modification and in the control of conversions between these modifications, because the free energy required for the formation of 2 = D nuclei is lowered by the presence of an appropriate substrate. Quantitatively, this is described by the following equation (42, 43):

$$\Delta G_s = \gamma_{12}A_{12} + (\gamma_{23} - \gamma_{13})A_{23} \quad (15)$$

where γ is the interaction energy per area, A is the surface area of the interfaces, and the subscript 3 represents the substrate. The total change in surface free energy will be lowered by favorable surface interactions between the aggregate and the substrate and unfavorable interactions between the crystallization medium and the substrate, due to the negative value of the second term in Equation (15). Consequently, increasing the surface area of the substrate will enhance nucleation.

The effectiveness of crystal seeding in controlling crystallization outcomes relies on the potential of crystal surfaces to promote heterogeneous or secondary nucleation (7, 8) while avoiding heterogeneous nucleation mediated by unknown contaminants. A review by Ward (44) on the structure, properties, and reactivity of organic crystal surfaces is recommended to develop strategies for the choice of surfaces that promote nucleation. Various studies (45–49) have demonstrated the influence of substrate topography, lattice parameters, crystallographic symmetry, and intermolecular interactions on surface-directed nucleation.

Heterogeneous nucleation mechanisms can significantly affect dissolution of metastable solid phases because this form of nucleation can occur at low driving forces. Whereas the choice of a metastable solid phase with a solubility higher than other crystalline modifications is motivated by the expectation of faster dissolution rates, achievement of faster dissolution rates and higher concentrations in solutions is jeopardized by surface-mediated nucleation. We have reported (47) that the surface of the metastable phase of theophylline promoted the nucleation of the stable monohydrate crystals. The observed oriented growth of monohydrate crystals on the anhydrous surface is consistent with a close lattice match between the **b** and **c** crystallographic axes (47). Other studies on the dissolution of metastable solids, such as anhydrous theophylline (50) and anhydrous carbamazepine (51–53), have shown that crystallization of the stable phase occurs during dissolution (Fig. 7). It is unfortunate that, in view of the important influence that nucleation mechanisms have on dissolution of metastable solid phases, very seldom are studies carried out to identify the potential of substrate-mediated nucleation by the metastable modification. The information gained from this

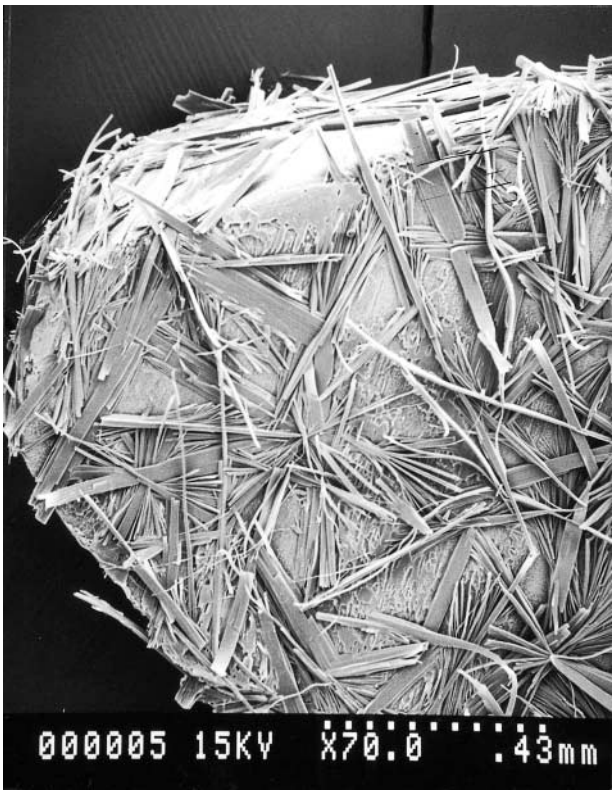


**Fig. 7** Nucleation and growth of dihydrate carbamazepine on crystal faces of anhydrous monoclinic carbamazepine in aqueous solutions of sodium lauryl sulfate (17.3 m*M*, 0.5%), *C*/*S* = 1.15 at 25°C. (From Ref. 136.)

type of study can be used in the design of methods to regulate crystallization during dissolution as well as during isolation of the desired solid form.

Carter and Ward (43) have identified a surface-mediated nucleation mechanism that involves a geometric shape match between planes of a ledge site on the substrate and planes of prenucleation aggregates. They have applied these concepts to the directed nucleation of polymorphs (45, 48). This work provides us with the attractive possibility that "a library of organic seeds can be used to control polymorphism, or to search for unknown polymorphs" (44). Molecular interpretations based on this approach are experimentally more accessible than those based on solvent-selective polymorph crystallization.

### Experimental and Computational Strategies

Whereas nucleation phenomena have their origin at the molecular level, they are often described in terms of macroscopic properties due to the scarcity of experimental techniques that allow for monitoring events at the molecular level. Nevertheless, information about molecular association processes in supersaturated systems obtained by laser Raman spectroscopy and laser light scattering has been used to identify prenucleation clusters and growth units under well-defined experimental conditions. Methods that measure cluster size distributions are more appropriate for studying crystallization of macromolecules (54–58) due to the large sizes of prenucleation clusters, whereas Raman and fluorescence spectroscopic techniques are capable of providing information about the solution structure or the species present in solution (59–63). The implications for crystallization pathways are examined by comparing the solution and crystal structures at a molecular level and by combining information obtained from macroscopic analysis with results from molecular simulations (64–74).

Gavezzotti (75–78) and Desiraju (79–81) have described crystal engineering strategies to understand the molecular aggregation processes involved in crystallization and to elucidate the supramolecular motifs in organic crystals. In this context, crystals are viewed as solid-state supermolecules assembled by intermolecular interactions, with the basic approach of establishing a relation between molecular interactions and supramolecular structure. Recent studies by Gavezzotti (78) show how molecular dynamics calculations allow for simulation of solvent and kinetic effects on molecular aggregation.

The supramolecular assembly process can be controlled so that the precursor nuclei in solution adopt a structure that resembles the structure of the desired crystalline modification (78, 82, 83). This concept has been used in the design of nucleation inhibitors to prevent growth of the stable polymorph and enhance the growth of the metastable polymorph (29, 84, 85). Davey et al. (64) have explained the solvent-dependent polymorph appearance of sulfathiazole by analyzing the intermolecular interactions in the various polymorphic structures and comparing them with the supramolecular assemblies that could exist in the different solvents. In this case, however, the solvent–dependent selective crystallization of a polymorph was not correlated with solubility (64, 86).

## CRYSTAL GROWTH

As stable nuclei (those larger than the critical cluster size) form, they grow into macroscopic crystals. This portion of the crystallization process is known as crystal growth. This process consists of several stages through which the growth units (i.e., the crystallographic basis that is "tacked onto" the space lattice to form the crystal structure) pass. These include: (1) transport of the growth unit from or through the bulk solution to an impingement site, which is not necessarily the final growth site, (2) adsorption of the growth unit at the impingement site, (3) diffusion of the growth units from the site of impingement to a growth site, and (4) incorporation into the lattice.

Desolvation of the growth unit may occur anywhere in steps 2–4, or the solvent may be adsorbed with the growth unit. Because any of these steps can be the rate-limiting step in the crystal growth process and they are dependent on conditions such as supersaturation, temperature, additives or solvent, and the hydrodynamics of the system, crystal growth is generally divided into two main mechanisms: volume-diffusion controlled or surface-integration controlled (Fig. 8) (6–9).

Crystal growth is volume-diffusion controlled when the diffusion of molecules from the bulk to the crystal surface is the rate-limiting step whereas growth is considered surface-integration controlled if the incorporation of a growth unit into the lattice is the slowest process. Many crystallization studies involving proteins, small organic electrolytes, and nonelectrolytes have reported growth controlled by surface-integration (71–73, 87–94). The roughness of the crystal surface determines whether growth occurs by the continuous (relatively rough surfaces) or the layer (relatively smooth surfaces) mechanism.

Crystal growth by the layer growth mechanism describes the formation of steps (i.e., layers) by two different mechanisms—2-D nucleation and screw dislocation. The model for 2-D nucleation was developed by

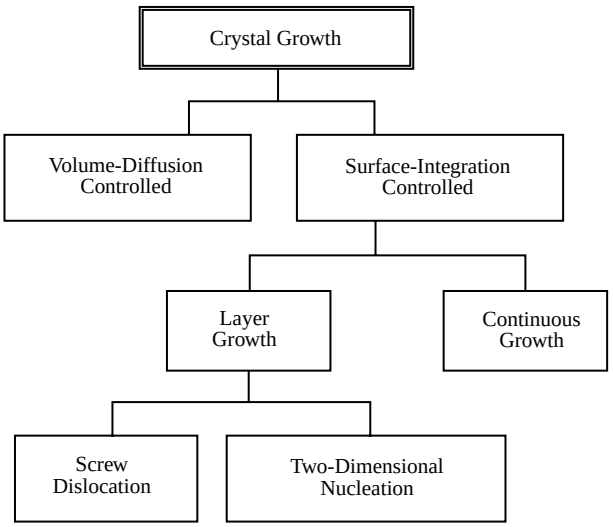


**Fig. 8** Mechanisms for crystal growth.

Volmer (95) and Stranski (96). The screw dislocation model was first described by Burton, Cabrera, and Frank (BCF;97). The details of the derivations for these models have been summarized in a number of other references (7, 9, 98, 99).

Two-dimensional nucleation occurs when nuclei at the crystal surfaces act as sources of steps that allow for the further incorporation of growth units. In general, this mechanism accounts for the crystal growth observed at high supersaturations. The screw dislocation mechanism often accounts for growth at lower supersaturations. When the supersaturation is below the threshold for formation of 2-D nuclei, the presence of screw dislocations provides a source of steps for the addition of growth units in an infinite sequence of equidistant and parallel steps.

## Experimental Strategies

Depending on the objectives and applications of growth rate measurements, the growth rate may be expressed as:

1. overall linear growth rate, which is the rate of change of the volume equivalent diameter with time;
2. linear growth rate of a face, which is the rate of displacement of a crystal face in a direction perpendicular to the face; and
3. velocity, height, and spacing of growth steps spreading across a crystal surface.

The linear growth rate of a face can be expressed in terms of the step velocity, step height, and step spacing. Techniques used for in situ measurement of crystal growth rates as a function of supersaturation include monitoring:

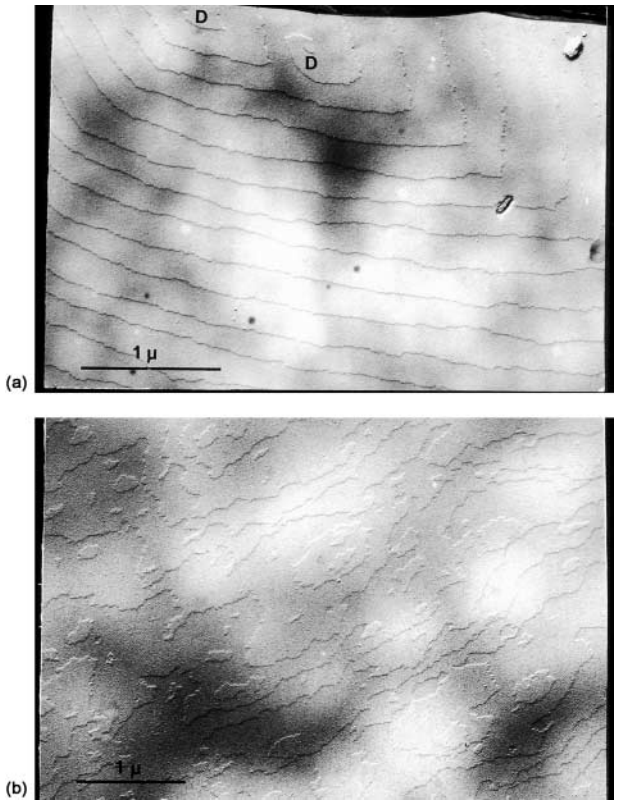


**Fig. 9** Surfaces of human insulin crystals showing that steps arise by different mechanisms depending on supersaturation. (a) At low supersaturation, steps are created by screw dislocations, D. (b) At high supersaturations, $c/s > 10$, steps occur at the edges of islands as a consequence of 2-D nucleation. (From Ref. 136.)

1. the crystal population by methods that measure particle size and number (100, 101);
2. the growth rates of individual crystal faces by optical microscopy with the use of a flow cell system (73, 87–90); and
3. the development of surface topography at the molecular level by atomic force microscopy (AFM 89, 91–94) and interferometric microscopy (71, 72).

Although various mathematical models have been used to identify the growth mechanism by fitting various equations to the experimentally measured face-growth rate dependence on supersaturation, it may be difficult to discriminate between mechanisms (73, 89, 102). This approach is often combined with examination of the surface topography to confirm the growth mechanism, as shown for human insulin crystals in Fig. 9. Monitoring the development of surface topography and transport processes during crystal growth will reveal events that are not evident from monitoring growth rates with optical microscopy. For instance, interactions of growth units

and additives with different crystal planes exposed on a surface may be deduced from the shape of 2-D nuclei and the kinetic anisotropy of the growth steps along crystallographic directions. These techniques have been successfully applied for identifying the crystal growth mechanisms and kinetics of small molecules (71, 72, 89) and proteins (91–94, 103).

## CRYSTAL MORPHOLOGY

Crystal growth is governed by both internal and external factors. Internal factors, such as the 3-D crystal structure and crystal defects, will determine the nature and strength of the intermolecular interactions between the crystal surface and the solution; whereas external factors, such as temperature, supersaturation, solvent, and the presence of impurities, will affect the type of interactions at the solid–liquid interface. The external shape or morphology of a crystal is a consequence of the relative growth rates of the faces, with the slowest growing faces impacting the crystal morphology to the largest extent. Examination of crystal morphology can reveal the molecular events occurring at the crystal face–liquid interfaces during growth. Consequently, even when morphology does not play a significant role in quality control, studying it is essential to understand the kinetics of crystallization (104).

### Crystal Structure and Nomenclature

Crystals are comprised of the long-range, 3-D periodic order of atoms held together through intramolecular covalent and ionic bonds and intermolecular noncovalent bonds. It is this long-range order that differentiates a crystalline solid from a glassy or amorphous solid which only demonstrates periodic order over a short range of atoms. When a chemical entity exists in more than one crystalline state—polymorph or solvate—each of these forms will have a different arrangement of atoms in the 3-D structure. Consequently, in addition to different physical and chemical properties, each of these forms has a unique crystal structure.

Considering the crystal from a purely geometric view (i.e., ignoring the exact arrangement of atoms), each crystal can be described by the smallest repeating translational unit in three dimensions, known as the unit cell. A unit cell is a parallelepiped, which can itself be described by six geometric measurements, three axes (designated "*a*," "*b*," and "*c*") and the angles between these axes (designated "α," "β," and "γ"), known as the lattice parameters. The relationship between the six lattice parameters defines to which of the seven unique crystal systems a particular crystal belongs (Table 3). Whereas the crystal system describes the geometric arrangement of the unit cell, the space group describes the individual translational and symmetrical relationships of the actual atoms within the unit cell. The combination of the lattice parameters, crystal system, space group and, ultimately, the individual atomic coordinates defines each unique crystal structure that exists for a crystalline solid. An example of the unit cell (with lattice parameters) and atomic coordinates for an anhydrous polymorph of the drug carbamazepine is shown in Fig. 10. This polymorph belongs to the monoclinic crystal system and the $P2_1/n$ space group (105).

**Table 3** Crystal systems and lattice parameters

| System | Relationship between lattice parameters |
|---|---|
| Cubic | $a = b = c$<br>$\alpha = \beta = \gamma = 90°$ |
| Tetragonal | $a = b \neq c$<br>$\alpha = \beta = \gamma = 90°$ |
| Orthorhombic | $a \neq b \neq c$<br>$\alpha = \beta = \gamma = 90°$ |
| Rhombohedral (or Trigonal) | $a \neq b \neq c$<br>$\alpha = \beta = \gamma \neq 90°$ |
| Hexagonal | $a = b \neq c$<br>$\alpha = \beta = 90°, \gamma = 120°$ |
| Monoclinic | $a \neq b \neq c$<br>$\alpha = \gamma = 90°, \beta \neq 90°$ |
| Triclinic | $a \neq b \neq c$<br>$\alpha \neq \beta \neq \gamma \neq 90°$ |

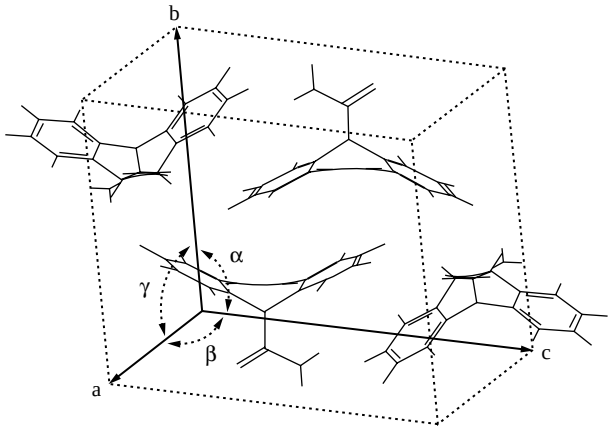


**Fig. 10** Unit cell of anhydrous monoclinic carbamazepine. Lattice parameters are marked with "a," "b," "c," "α," "β," and "γ." (From Ref. 105.)

**Table 4** Nomenclature for anhydrous carbamazepine polymorphs

| | CBZ(AM) | CBZ(ATrg) | CBZ(ATrc) | Reference |
|---|---|---|---|---|
| Crystal system | Monoclinic | Trigonal | Triclinic | |
| $T_{melt}$ | 175–180°C | 192–194°C | 192–195°C | |
| Nomenclature | III | | I | 106–109 |
| | I | II | III | 110–112 |
| | beta | alpha | | 113 |
| | monoclinic | trigonal | | 114 |
| | | | triclinic | 115 |

The convention of Miller indices is used to describe the planes within a unit cell. Miller indices are defined as the reciprocals of the intercept which the plane makes with each of the three crystal axes. Each plane is denoted by three parameters "*h*," "*k*," and "*l*." Planes that are parallel to a crystal axis are given the Miller index of 0, whereas planes formed in the negative direction are written with a bar over the number in the Miller index. The Miller index of a single specific plane is written within parentheses (*hkl*), whereas the Miller indices describing a whole family of faces are written with braces {*hkl*}. The faces that exist and define the crystal morphology are termed morphologically important and are commonly identified by the Miller indices of the planes represented by those faces.

The use of nomenclature indicative of the crystal structure would alleviate much of the confusion that exists in the literature when describing different polymorphs or solvates. Whereas it is often convenient to use terminology such as "Form I and Form II" or "α-form versus β-form," this can lead to confusion when different investigators use inconsistent or, in some cases, conflicting nomenclature to describe the same polymorphic forms. For instance, carbamazepine has been shown to exist in at least three anhydrous forms and two solvated forms (a dihydrate and an acetonate). Overlapping or conflicting nomenclature has been used when describing the three anhydrous forms and has led to much confusion (Table 4) (106–115). As can be seen, nomenclature arising from crystallographic information (in this case, crystal system) would be more meaningful and less confusing than the commonly used terminology.

## The Role of Crystal Morphology in Pharmaceutical Processes

Knowledge of crystal morphology and ways to control and predict the morphology of drugs and excipients could prove invaluable in processing and product development. In a review on solid-state properties of powders, York has discussed how changes in crystal morphology can affect several formulation parameters, such as particle size distribution, powder flow, mixing (and agglomeration), dissolution, compression, and tablet hardness (116). Crystal morphology could also impact the rheology and filtration of suspensions. Additionally, certain crystal habits may lead to lack of dose uniformity or erratic drug delivery, as is the case with aerosols where particle size is critical for delivery (117–119). It should also be emphasized that the effect of crystal morphology does not impact the active ingredient solely. Because excipients often comprise much larger percentages of the formulation, the crystal morphology of each component may have profound effects on the characteristics previously described.

Often during processing or delivery of a formulation, supersaturated states are created, which may lead to the crystallization of drug or excipient. Consequently, the interactions between drugs and excipient (or excipient–excipient interaction) could have a tremendous impact on the morphology. In the strictest sense, the excipient is an impurity with respect to the active ingredient (or vice versa) and may result in changes in the crystal morphology that could adversely effect both processing and/or delivery.

The presence of additives (intentional) or impurities (unintentional) have long been known to have a significant impact on crystallization (both nucleation and growth; 7, 9). If an additive (or impurity) selectively adsorbs to a crystal face, the growth rates of those faces will be altered resulting in a change in crystal morphology. For example, interaction of sodium taurocholate (STC) with the {111} faces of carbamazepine dihydrate (CBZ(D)) decreases the growth rate along the needle axis and results in more prismatic crystals (Fig. 11) (53, 120). Photomicrographs demonstrating the effects of STC on CBZ(D) morphology are seen in Fig. 12. Lechuga-Ballesteros and Rodríguez-Hornedo have shown how the adsorption of hydrophobic L-amino acids can inhibit the growth rate of the {012} faces of L-alanine resulting in a change in crystal morphology (89, 90, 101, 121). The presence of structurally similar additives has also been shown to significantly change the crystal

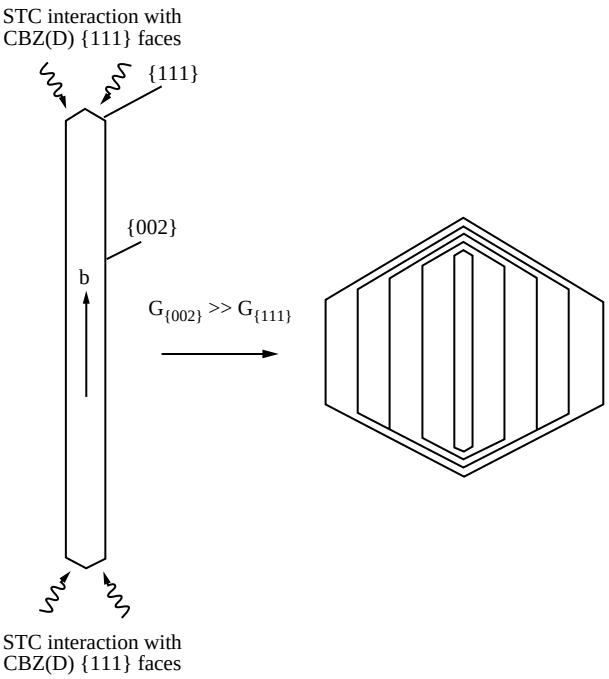


**Fig. 11** Two-dimensional representation of the effect of sodium taurocholate (STC) on the crystal morphology of dihydrate carbamazepine (CBZ(D)). STC interacts specifically with the {111} faces of CBZ(D), resulting in inhibition of the growth of those faces and changing the morphology from needles to prisms.

morphology of paracetamol (70). Recently, there has been much work exploiting the selective interaction of additives with crystal faces in order to "tailor" the crystal morphology to a more favorable habit (122).

Monitoring the changes in morphology by visual examination can be a powerful tool when troubleshooting formulation problems. The appearance of crystals with different morphology is indicative of changes in the processing conditions, such as in the degree of supersaturation, rate of heating or cooling, or the presence (or absence) of impurities. Changes in morphology could also be the first suggestion of the appearance of a new crystal form (polymorph or solvate). Characterization techniques, such as x-ray powder diffraction, thermal analysis, or spectroscopy, can be used to identify the appearance of new forms first identified by observing changes in morphology.

## Morphology Prediction and Other Computational Strategies

With the objective of predicting the morphology of crystals, several models have been developed. One of the first models for predicting crystal morphology is based on the general Law of Bravais (123), which states that crystal faces with the most morphological importance have the greatest interplanar distance, $d_{hkl}$. The Bravais–Friedel Donnay–Harker (BFDH) model predicts that the morphological importance of a face is proportional to the interplanar spacing corrected for extinction conditions and translational repetitions of the crystal space group (123–125). Consequently, the growth rate of any given face is inversely proportional to its interplanar spacing:

$$G_{hkl} \propto \frac{1}{d_{hkl}} \tag{16}$$

where $G_{hkl}$ is the growth rate of a face and $d_{hkl}$ is the interplanar spacing. This model has been used to predict the morphology for many small molecules including compounds of pharmaceutical interest. (3, 73, 120, 126, 127). The observed (Fig. 13a) and predicted morphology (Fig. 13b) of carbamazepine dihydrate shows that the BFDH model correctly predicts the axis of elongation as well as the appearance of the {002}, {200}, and {111} faces. This model, however, did not correctly predict the aspect ratio of the crystal because it is based on geometric parameters solely. It considers neither molecular interactions nor the effect of anisotropic forces, such as intermolecular hydrogen bonding or $\pi-\pi$ interactions.

Early work by Hartman and Perdok (128) described crystal growth in terms of the formation of strong bonds between neighboring crystallizing units. Uninterrupted straight chains of these bonds were classified as periodic bond chains (PBC). This theory led to the classification of three types of crystal faces: F-faces (flat), S-faces (stepped), and K-faces (kinked), based on the number of PBCs in a slice thickness, $d_{hkl}$. K-faces, which had no PBCs present in a slice were shown to be the fastest growing, whereas the F-faces, which had two or more PBCs, grew the slowest. Consequently, the F-faces were the most morphologically important faces. The PBC theory ultimately led to the development of the attachment energy (AE) model (122, 129) which states that the growth rate of a face, $G_{hkl}$, is proportional to its attachment energy, $E_{\text{att}}$:

$$G_{hkl} \propto E_{att} \tag{17}$$

where the attachment energy can be defined as the energy released when one growth layer ($d_{hkl}$) crystallizes on the surface of a crystal. The attachment energy can be calculated as the difference between the energy of crystallization (or lattice energy) and the energy of a growth slice:

$$\mathrm{E}_{att} = \mathrm{E}_{crystal} - \mathrm{E}_{slice} \tag{18}$$

The values for the energy of crystallization can be calculated by summation of the intermolecular interactions

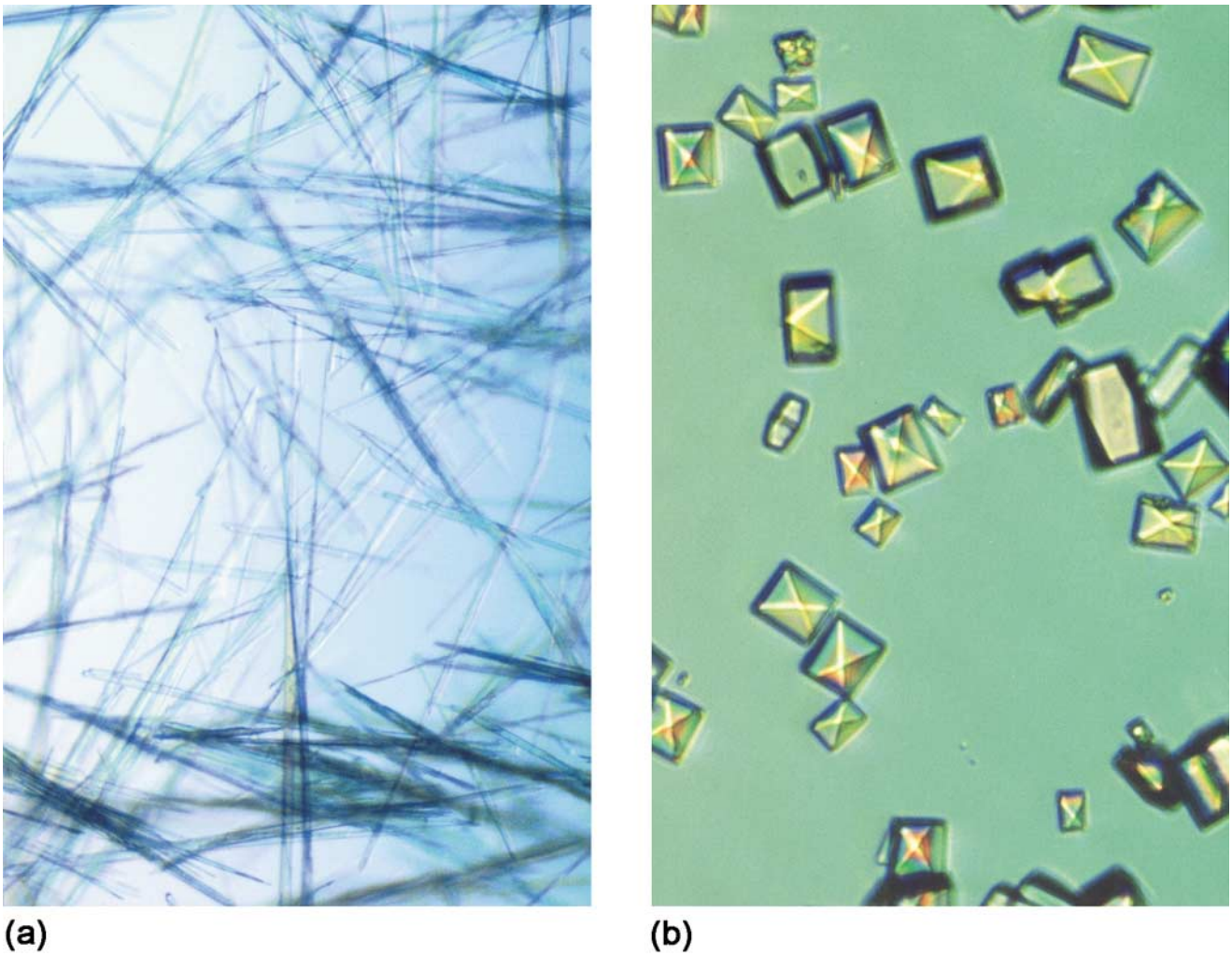


**Fig. 12** Photomicrographs of CBZ(D) crystals grown in aqueous solutions $C/S = 2.5$ at 25°C. (a) In the absence of surfactant. (b) In the presence of 9 m*M* STC. (From Ref. 53.)

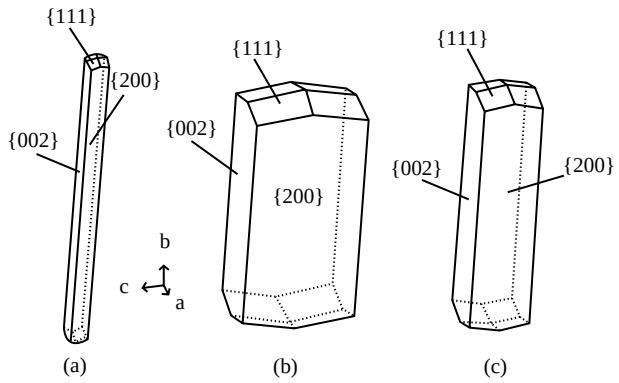


**Fig. 13** Dihydrate carbamazepine morphology: (a) Observed morphology when grown from water, (b) Predicted by the BFDH model, (c) Predicted by the AE model. (From Ref. 53.)

from a central reference molecule and all other molecules within the crystal. Similarly, the energy of a growth slice can be calculated for all molecules in that particular slice.

The AE method has been used to successfully predict the morphology for many molecular crystals, especially those that are dominated by strong anisotropic forces (3, 73, 120, 126, 127). In the case of carbamazepine dihydrate, which is dominated by intermolecular hydrogen bonding (especially along the **b**- axis), this model predicts a morphology much closer to the observed morphology (Fig. 13c) (53). Whereas this method can account for anisotropic forces, predictions are very dependent on the force field chosen to calculate the nonbond intermolecular interactions. Much care should be given to the choice of appropriate force fields for the molecules in question. The force field developed by Lifson and coworkers (130),

which is explicitly parameterized for C, H, N, and O atoms, was used in the AE method prediction of carbamazepine dihydrate (53).

Morphology predictions based on the AE method also assume that crystals are grown in vacuo, i.e., in the absence of solvent. Consequently, the solvent effects on morphology are ignored using this method. Roberts et al. have developed a method that calculates a modified attachment energy that can be used to predict the effects of solvents as well as other additives on crystal morphology (131).

With knowledge of the crystal structure, morphology, and intermolecular interactions present, strategies have been developed for the rational choice of additives that will specifically inhibit the growth of the stable polymorph and enhance the growth of a metastable polymorph (29, 64, 65, 74, 84–85, 132–134). These strategies can also be applied to systems for which a change in crystal morphology is desired to aid in product development or delivery (e.g., creating a prismatic habit when a crystal grows preferentially as a needle). The main features of these strategies are:

1. identification of the fastest growing faces of the stable crystalline modification (from experimental data as well as morphology predictions);
2. characterization of intermolecular interactions along the crystallographic direction with fastest growth;
3. selection of additives that can be incorporated into (or adsorbed onto) the crystalline structure along this direction; and
4. development of experimental methods to investigate the effectiveness of the additive to kinetically stabilize the metastable modification.

The selection of additives can be guided by molecular visualizations of the crystal structure based on geometric fits (29, 90) or binding energy calculations (70, 120, 135).

## SOLUTION-MEDIATED TRANSFORMATIONS

Knowledge of the propensity of a metastable solid phase to dissolve in a liquid phase from which a stable solid phase nucleates and grows is crucial in many stages of pharmaceutical development. This is because pharmaceutical solids are designed to be dissolved and to come in contact with solvents from the early stages of development (isolated by crystallization from solution) and during processing (wet granulation, spray-drying, freeze-drying, etc.). Given that the sudden disappearance or appearance of a crystalline modification can threaten process development, characterization of the kinetics and mechanisms of solvent-mediated transformations is of practical importance. It will provide answers to questions such as: What is the relation between processing conditions and the solid-state modification manufactured? Is there a correlation between dissolution conditions, solid phase(s) dissolving, and concentration of drug dissolved?

The importance of phase transition kinetics, molecular interpretations, and process implications are emphasized by several investigators (29–31, 47, 64, 133, 136–138). Cardew and Davey (30) developed a theoretical framework to investigate solvent-mediated transformations in terms of dissolution kinetics of one phase and growth of a second phase. The model represents the time development of the supersaturation with respect to the stable phase, or solute concentration in solution, and to the solid phase composition during the transformation. This experimental approach involves saturating the solution with respect to the metastable phase under consideration and to monitor both solution concentration and solid phase composition in the presence of the metastable phase, under constant external conditions. More useful information is obtained from the concentration or supersaturation profiles than from the solid phase composition profiles with time because the former is related to the driving forces that regulate the transformation rate and can be used to identify the rate-controlling process: dissolution or growth. A calculated supersaturation profile with growth-limited and dissolution-limited regimes is shown in Fig. 14 for the case in which dissolution and growth are linearly dependent on supersaturation (30, 31). Experimental studies of the phase transitions of organic crystals have shown this model to be applicable in explaining the solution-mediated transformation kinetics of polymorphs (30, 31, 138) and solvents (47) and to be applicable to process development (138).

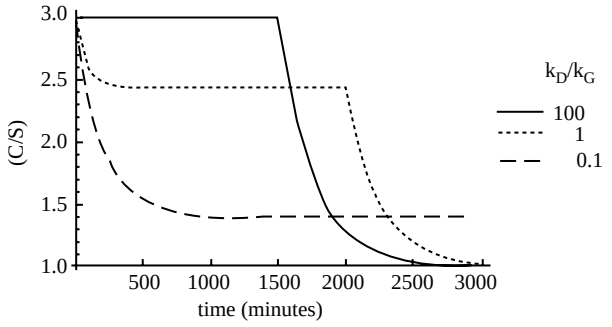


**Fig. 14** Simulation of the supersaturation–time profiles as a function of the relative rates of dissolution and crystallization during a solution–mediated transformation. Generated from a kinetic model developed by Cardew and Davey (30), assuming that both dissolution and growth rates are linearly dependent on their respective driving forces. (Adapted from Ref. 136.)

**Table 5** Information on crystallization kinetics and mechanisms provided by various experimental techniques

| Techniques | Information |
|---|---|
| Optical microscopy (inverted microscope) | Study crystallization processes in situ<br>Monitor transformations in suspensions<br>Determine transformation times<br>Screen and characterize additive/solvent interactions with specific crystal faces<br>Identify nucleation mechanisms<br>Measure crystal growth rates |
| Electron microscopy | Characterize additive/solvent interactions with specific crystal faces<br>Identify nucleation and growth mechanisms |
| Atomic force microscopy | Study crystallization processes in situ |
| Interferometric microscopy | Examine surface topography<br>Identify nucleation and growth mechanisms<br>Measure crystal growth rates |
| Raman spectroscopy | Monitor molecular association processes that direct nucleation and crystal growth |
| Infrared (FT-IR, NIR) spectroscopy, solid-state NMR Spectroscopy | Monitor structure (polymorphs and solvates), conformation, and intermolecular environment of crystals |
| Spectrophotometry, chromatography | Monitor concentration of solute in solution and supersaturation |
| Diffraction, Calorimetry, Spectroscopy | Monitor solid phase composition |

Some useful experimental techniques for studying small and large scale crystallization and solution-mediated transformations are summarized in Table 5.

## SUMMARY

In this chapter, we have discussed the significance of crystallization mechanisms and kinetics in directing crystallization pathways and have presented numerous examples that confirm the importance of controlling the crystallization events (both nucleation and growth) in the pharmaceutical industry. Advances in computational and analytical techniques now provide access to the molecular events that direct nucleation and crystal growth. Consequently, there is no reason for the development of ill-defined crystallization processes even when the desired product is obtained. Understanding the thermodynamic and kinetic behavior of the system is vital for the design of reliable processes; thus, at least a holistic approach that identifies the relevant experimental parameters is essential. Whereas the objectives of formulation or process development may not explicitly include interpretations at the molecular level, the information concealed in the interfaces present during the process, the structure of solutions, and the solids harvested can be significant in the identification of nucleation and growth mechanisms. However, there may be instances, such as the unintentional isolation of a new crystal structure or morphology with poor formulation characteristics, where knowledge of the molecular level events could prove invaluable in solving formulation or processing problems. Although the significance of crystallization mechanisms and kinetics has been underestimated in the pharmaceutical industry, we hope that the recent developments in computational and analytical techniques will inspire interest in their application to pharmaceutical systems.

## ACKNOWLEDGMENTS

The authors acknowledge financial support from the National Science Foundation, the Pharmaceutical Research and Manufacturers of America Foundation, Inc., Fellowship for Advanced Predoctoral Training in Pharmaceutics, the Valteich Research Award, and the Fred W. Lyons, Jr., Fellowship from the University of Michigan College of Pharmacy.

## REFERENCES

1. Dunitz, J.D.; Bernstein, J. Disappearing Polymorphs. Acc. Chem. Res. **1995**, *28*(4), 193–200.
2. Abbott Laboratories. Letter to Health Care Providershttp://www.fda.govv/medwatch/ safety/1998/ norvir.htm (accessed Mar 2000).
3. Nichols, G.; Frampton, C.S. Physicochemical Characterization of the Orthorhombic Polymorph of Paracetamol Crystallized from Solution. J. Pharm. Sci. **1998**, *87*, 684–692.

4. Haisa, M.; Kashino, S.; Maeda, H. The Orthorhombic Form of P-Hydroxyacetanilide. Acta. Crystallogrn. **1974**, B*30*, 2510–2512.
5. Food and Drug Administration. *Guideline for Submitting Supporting Documentation in Drug Applications for the Manufacture of Drug Substances*; FDA Center for Drug Evaluation and Research; Office of Drug Evaluation: Rockville, Maryland, 87.
6. Nyvlt, J.; Söhnel, O.; Matuchová, M.; Broul, M. *The Kinetics of Industrial Crystallization*; Elsevier: New York , 1985.
7. Mullin, J.W. *Crystallization*; Butterworth-Heinemann Ltd., Oxford, 1993.
8. Söhnel, O.; Garside, J. *Precipitation: Basic Principles and Industrial Applications*; Butterworth-Heinemann Ltd.: Oxford, 1992.
9. Myerson, A.S. *Handbook of Industrial Crystallization*; Butterworth-Heinemann Ltd.: Oxford, 1993.
10. Mersmann, A. *Crystallization Technology Handbook*; Marcel Dekker, Inc.: New York, 1995.
11. Van den Berg, L. The Effect of Addition of Sodium and Potassium Chloride to the Reciprocal System: $KH_2PO_4$–$NA_2HPO_4$–$H_2O$ on pH and Composition during Freezing. Arch. Biochem. Biophys. **1959**, *84*, 305–315.
12. Van den Berg, L. PH Changes in Buffers and Foods During Freezing and Subsequent Storage. Cryobiology, **1966**, *3*, 236–242.
13. Larsen, S.S. Studies on Stability of Drugs in Frozen Systems VI: The Effect of Freezing upon PH for Buffered Aqueous Solutions. Arch. Pharm. Chemi. Sci. Ed. **1973**, *1*, 41–53.
14. MacKenzie, A.P. Non-equilibrium Freezing Behaviour of Aqueous Systems. Philos. Trans. R. Soc. London, Ser. B. **1977**, *278*, 167–189.
15. Taylor, M.J. Physico-Chemical Principles in Low Temperature Biology. *The Effects of Low Temperatures on Biological Systems*; Grout, B.W.W., Morris, G.J., Eds.; E. Arnold: London, 1987; 1–71.
16. Murase, N.; Franks, F. Salt Precipitation during the Freeze-Concentration of Phosphate Buffer Solutions. Biophys. Chem. **1989**, *34*(3), 293–300.
17. Gómez, G. *Crystallization-related pH Changes during Freezing of Sodium Phosphate Buffer Solutions*; University of Michigan: Ann Arbor, MI, 1995.
18. Zettlemoyer, A.C. *Nucleation*; Marcel Dekker, Inc.: New York, 1969.
19. Perepezko, J.H. Nucleation Reactions in Undercooled Liquids. Materials Science and Engineering A-Structural Materials Properties Microstructure and Processing. **1994**, *178*(1–2), 105–111.
20. Perepezko, J.H. Kinetic Processes in Undercooled Melts. Materials Science and Engineering A-Structural Materials Properties Microstructure and Processing. **1977**, *226*, 374–382.
21. Gibbs, J.W. *Collected Works*; Vol. I. Thermodynamics Yale University Press: New Haven, 1948.
22. Volmer, M. *Kinetic Der Phasenbildung*; Steinkopff: Leipzig, 1939.
23. Becker, R.; Döring, W. Kinetische Behandlung Der Keimbildung in Übersättigen Dämpfen. Annalen Der Physik **1935**, *24*, 719–752.
24. Turnbull, D.; Fisher, J.C. Rate of Nucleation in Condensed Systems. J. Chem. Phys. **1949**, *17*, 71–3.
25. Boistelle, R.; Astier, J.P. Crystallization Mechanisms in Solution. J. Cryst. Growth **1988**, *90*, 14–30.
26. Hendriksen, B.A.; Grant, D.J.W. The Effect of Structurally Related Substances on the Nucleation Kinetics of Paracetamol (Acetaminophen). J. Cryst. Growth **1995**, *156*, 252–260.
27. Garti, N.; Tibika, F. Habit Modifications of Nitrofurantoin Crystallized from Formic Acid Mixtures. Drug Dev. Ind. Pharm. **1980**, *6*, 379–398.
28. Ostwald, W. Studien Über Die Bildung Und Umwandlung Fester Körper. Zieitschrigt Für Physikalische Chemie **1897**, *22*, 289–330.
29. Davey, R.J.; Blagden, N.; Potts, G.D.; Docherty, R. Polymorphism in Molecular Crystals: Stabilization of a Metastable Form by Conformational Mimicry. J. Am. Chem. Soc. **1997**, *119*(7), 1767–1772.
30. Cardew, P.T.; Davey, R.J. The Kinetics of Solvent-Mediated Phase Transformations. Proc. R. Soc. Lond. Ser. A **1985**, *398*, 415–428.
31. Davey, R.J.; Cardew, P.T.; Mcewan, D.; Sadler, D.E. Rate Controlling Processes in Solvent-Mediated Phase Transformations. J. Crys. Growth **1986**, *79*, 648–653.
32. Pellett, M.A.; Castellano, S.; Hadgraft, J.; Davis, A.F. The Penetration of Supersaturated Solutions of Piroxicam Across Silicone Membranes and Human Skin In Vitro. J. Controlled Release **1997**, *46*(3), 205–214.
33. Katzhendler, I.; Azoury, R.; Friedman, M. Crystalline Properties of Carbamazepine in Sustained Release Hydrophilic Matrix Tablets Based on Hydroxypropylmethylcellulose. J. Controlled Release **1998**, *54*(1), 69–85.
34. Davey, R.J.; Hilton, A.M.; Garside, J. Crystallization from Oil in Water Emulsions: Particle Synthesis and Purification of Molecular Materials. Chem. Eng. Res. Des. **1997**, *75*(A2), 245–251.
35. Davey, R.J.; Garside, J.; Hilton, A.M.; Mcewan, D.; Morrison, J.W. Purification of Molecular Mixtures below the Eutectic by Emulsion Crystallization. Nature **1995**, *375*(6533), 664–666.
36. Davey, R.J.; Garside, J.; Hilton, A.M.; Mcewan, D.; Morrison, J.W. Emulsion Solidification of Meta–Chloronitrobenzene: Purification and Crystallisation. J. Cryst. Growth **1996**, *166*(1–4), 971–975.
37. Turnbull, D. Under what Conditions can a Glass be Formed? Contemp. Phys. **1969**, *10*, 473–488.
38. Murase, N.; Echlin, P.; Franks, F. The Structural States of Freeze-Concentrated and Freeze-Dried Phosphates Studied by Scanning Electron-Microscopy and Differential Scanning Calorimetry. Cryobiology **1991**, *28*(4), 364–375.
39. Cavatur, R.K.; Suryanarayanan, R. Characterization of Frozen Aqueous Solutions by Low Temperature X–ray Powder Diffractometry. Pharm. Res. **1998**, *15*(2), 194–199.
40. Mullin, J.W.; Leci, C.L. Some Nucleation Characteristics of Aqueous Citric Acid Solutions. J. Cryst. Growth **1969**, *5*, 75–76.
41. Franks, F.; Mathias, S.F.; Trafford, K. The Nucleation of Ice in Undercooled Water and Aqueous Polymer Solutions. Colloids Surf. **1984**, *11*, 275–285.
42. Fletcher, N.H. Nucleation by Crystalline Particles. J. Chem. Phys. **1963**, *38*, 237.

43. Carter, P.W.; Ward, M.D. Topographically Directed Nucleation of Organic-Crystals on Molecular Single-Crystal Substrates. J. Am. Chem. Soc. **1993**, *115*(24), 11521–11535.
44. Ward, M.D. Organic Crystal Surfaces: Structure, Properties and Reactivity. Curr. Opin. Colloid Interface Sci. **1997**, *2*(1), 51–64.
45. Carter, P.W.; Ward, M.D. Directing Polymorph Selectivity During Nucleation of Anthranilic Acid on Molecular Substrates. J. Am. Chem. Soc. **1994**, *116*(2), 769–770.
46. Black, S.N.; Bromley, L.A.; Cottier, D.; Davey, R.J.; Dobbs, B.; Rout, J.E. Interactions at the Organic Inorganic Interface—Binding Motifs for Phosphonates at the Surface of Barite Crystals. J. Chem. Soc., Faraday Trans. **1991**, *87*(20), 3409–3414.
47. Rodríguez-Hornedo, N.; Lechuga-Ballesteros, D.; Wu, H.J. Phase Transition and Heterogeneous Epitaxial Nucleation of Hydrated and Anhydrous Theophylline Crystals. Int. J. Pharm. **1992**, *85*(1–3), 149–162.
48. Bonafede, S.J.; Ward, M.D. Selective Nucleation and Growth of an Organic Polymorph by Ledge-Directed Epitaxy on a Molecular-Crystal Substrate. J. Am. Chem. Soc. **1995**, *117*(30), 7853–7861.
49. Davey, R.J.; Maginn, S.J.; Andrews, S.J.; Black, S.N.; Buckley, A.M.; Cottier, D.; Dempsey, P.; Plowman, R.; Rout, J.E.; Stanley, D.R.; Taylor, A. Morphology and Polymorphism in Molecular Crystals—Terephthalic Acid. J. Chem. Soc., Faraday Trans. **1994**, *90*(7), 1003–1009.
50. De Smidt, J.G.; Fokkens, J.G.; Grijseels, H.; Crommelin, D.A.J. Dissolution of Theophylline Monohydrate and Anhydrous Theophyline in Buffer Solutions. J. Pharm. Sci. **1986**, *75*, 497–501.
51. Luhtala, S.; Kahela, P.; Kristoffersson, E. Effect of Benzalkonium Chloride on Crystal Growth and Aqueous Solubility of Carbamazepine. Acta Pharmaceutica Fennica **1990**, *99*, 59–68.
52. Luhtala, S. Effect of Sodium Lauryl Sulfate and Polysorbate 80 on Crystal Growth and Aqueous Solubility of Carbamazepine. Acta Pharm. Nord. **1992**, *4*, 85–90.
53. Murphy, D. *The Solvent-Mediated Phase Transformation of Carbamazepine and the Influence of Surfactants on the Nucleation Mechanism and Crystal Morphology*; University of Michigan: Ann Arbor, MI, 1997.
54. Kadima, W.; McPherson, A.; Dunn, M.F.; Jurnak, F. Precrystallization Aggregation of Insulin by Dynamic Light–Scattering and Comparison With Canavalin. J. Cryst. Growth **1991**, *110*(1–2), 188–194.
55. Georgalis, Y.; Umbach, P.; Raptis, J.; Saenger, W. Lysozyme Aggregation Studied by Light Scattering 2. Variations of Protein Concentration. Acta Crystallogr. Sect. D—Biological Crystallography **1997**, *53*, 703–712.
56. Georgalis, Y.; Umbach, P.; Zielenkiewicz, A.; Utzig, E.; Zielenkiewicz, W.; Zielenkiewicz, P.; Saenger, W. Microcalorimetric and Small Angle Light Scattering Studies on Nucleating Lysozyme Solutions. J. Am. Chem. Soc. **1997**, *119*(49), 11959–11965.
57. Peters, R.; Georgalis, Y.; Saenger, W. Accessing Lysozyme Nucleation with a Novel Dynamic Light Scattering Detector. Acta Crystallogr. Sect. D—Biological Crystallography **1998**, *54*, 873–877.
58. Rosenberger, F.; Vekilov, P.G.; Muschol, M.; Thomas, B.R. Nucleation and Crystallization of Globular Proteins—What we Know and What is Missing. J. Cryst. Growth **1996**, *168*(1–4), 1–27.
59. Cerreta, M.K.; Berglund, K.A. The Structure of Aqueous–Solutions of Some Dihydrogen Ortho–Phosphates by Laser Raman-Spectroscopy. J. Cryst. Growth **1987**, *84*(4), 577–588.
60. Yedur, S.K.; Berglund, K.A. Use of Fluorescence Spectroscopy in Concentration and Supersaturation Measurements in Citric Acid Solutions. Appl. Spectrosc. **1996**, *50*(7), 866–870.
61. Rasimas, J.P.; Berglund, K.A.; Blanchard, G.J. Measuring Self Assembly in Solution: Incorporation and Dynamics of a ''Tailor–Made Impurity'' In Precrystalline Glucose Aggregates. J. Phys. Chem. **1996**, *100*(42), 17034–17040.
62. Rasimas, J.P.; Berglund, K.A.; Blanchard, J.G. A Molecular Lock and Key Approach to Detecting Solution Phase Self Assembly. A Fluorescence and Absorption Study of Carminic Acid in Aqueous Glucose Solutions. J. Phys. Chem. **1996**, *100*(17), 7220–7229.
63. Dunuwila, D.D.; Berglund, K.A. ATR FTIR Spectroscopy for In Situ Measurement of Supersaturation. J. Cryst. Growth **1997**, *179*(1–2), 185–193.
64. Blagden, N.; Davey, R.J.; Lieberman, H.F.; Williams, L.; Payne, R.; Roberts, R.; Rowe, R.; Docherty, R. Crystal Chemistry and Solvent Effects in Polymorphic Systems — Sulfathiazole. J. Chem. Soc., Faraday Trans. **1998**, *94*(8), 1035–1044.
65. Weissbuch, I.; Popovitzbiro, R.; Lahav, M.; Leiserowitz, L. Understanding and Control of Nucleation, Growth, Habit, Dissolution and Structure of 2-Dimensional and 3-Dimensional Crystals Using Tailor–Made Auxiliaries. Acta Crystallogr., Sect. B: Struct. Sci. **1995**, *51*, 115–148.
66. Leiserowitz, L.; Addadi, L.; Lahav, M. Macroscopic Phenomena in Crystals and Molecular Shape. J. Mol. Graphics **1989**, *7*(2), 95–5.
67. Weissbuch, I.; Addadi, L.; Lahav, M.; Leiserowitz, L. Molecular Recognition At Crystal Interfaces. Science **1991**, *253*(5020), 637–645.
68. Gallagher, H.G.; Roberts, K.J.; Sherwood, J.N.; Smith, L.A. A Theoretical Examination of the Molecular Packing, Intermolecular Bonding and Crystal Morphology of 2,4,6-Trinitrotoluene in Relation to Polymorphic Structural Stability. J. Mater. Chem. **1997**, *7*(2), 229–235.
69. Clydesdale, G.; Roberts, K.J.; Telfer, G.B.; Grant, W.D.J. Modeling the Crystal Morphology of Alpha–Lactose Monohydrate. J. Pharm. Sci. **1997**, *86*(1), 135–141.
70. Hendriksen, B.A.; Grant, D.J.W.; Meenan, P.; Green, A.D. Crystallisation of Paracetamol (Acetaminophen) in the Presence of Structurally Related Substances. J. Cryst. Growth **1998**, *183*(4), 629–640.
71. Shekunov, B.Y.; Lahtam, R. Growth Anisotropy Of *N*-Methylurea Crystals in Methanol. J. Phys. Chem. A **1996**, *100*, 5464–5469.
72. Shekunov, B.Y.; Grant, D.J.W. In Situ Optical Interferometric Studies of the Growth and Dissolution Behavior of Paracetamol (Acetaminophen) .1. Growth Kinetics. J. Phys. Chem. B **1997**, *101*(20), 3973–3979.
73. Zipp, G.L.; Rodríguez-Hornedo, N. Growth Mechanism and Morphology of Phenytoin and their Relationship with Crystallographic Structure. J. Phys. D: Appl. Phys. **1993**, *26*(8B), B48–B55.

74. Khoshkhoo, S.; Anwar, J. Study of the Effect of Solvent on the Morphology of Crystals Using Molecular Simulation: Application to Alpha-Resorcinol And *n-n*-Octyl-D-Gluconamide. J. Chem. Soc., Faraday Trans. **1996**, *92*(6), 1023–25.
75. Gavezzotti, A. Computer Simulations of Organic Solids and Their Liquid-State Precursors. Faraday Discussions **1997**, *106*, 63–77.
76. Gavezzotti, A.; Filippini, G. Polymorphic Forms of Organic Crystals at Room Conditions —Thermodynamic and Structural Implications. J. Am. Chem. Soc. **1995**, *117*(49), 12299–12305.
77. Gavezzotti, A.; Filippini, G. Computer Prediction of Organic Crystal Structures Using Partial X–ray Diffraction Data. J. Am. Chem. Soc. **1996**, *118*(30), 7153–7157.
78. Gavezzotti, A.; Filippini, G. Self-organization of Small Organic Molecules in Liquids, Solutions and Crystals: Static And Dynamic Calculations. Chem. Commun. **1998**, *3*, 287–294.
79. Desiraju, G.R. Supramolecular Synthons in Crystal Engineering—A New Organic–Synthesis. Angew. Chem., Int. Ed. Engl. **1995**, *34*(21), 2311–2327.
80. Desiraju, G.R. Crystal Gazing: Structure Prediction and Polymorphism. Science **1997**, *278*(5337), 404–405.
81. Desiraju, G.R. Designer Crystals: Intermolecular Interactions, Network Structures and Supramolecular Synthons. Chemical Communications **1997**, *16*, 1475–1482.
82. Boistelle, R.; López-Valero, I. Growth Units and Nucleation: The Case of Calcium Phosphates. J. Crys. Growth **1990**, *102*, 609–617.
83. Gidalevitz, D.; Feidenhansl, R.; Matlis, S.; Smilgies, D.M.; Christensen, M.J.; Leiserowitz, L. Monitoring in Situ Growth and Dissolution of Molecular Crystals: Towards Determination of the Growth Units. Angew. Chem., Int. Ed. Engl. **1997**, *36*(9), 955–959.
84. Weissbuch, I.; Leisorowitz, L.; Lahav, M. Tailor –Made and Charge–Transfer Auxiliaries for the Control of the Crystal Polymorphism of Glycine. Adv. Mater. **1994**, *6*(12), 952–956.
85. Weissbuch, I.; Zbaida, D.; Addadi, L.; Leiserowitz, L.; Lahav, M. Design of Polymeric Inhibitors for the Control of Crystal Polymorphism—Induced Enantiomeric Resolution of Racemic Histidine by Crystallization At 25 °C. J. Am. Chem. Soc. **1987**, *109*(6), 1869–1871.
86. Khoshkhoo, S.; Anwar, J. Crystallization of Polymorphs—The Effect of Solvent. J. Phys. D: Appl. Phys. **1993**, *26*(8B), B90–B93.
87. Li, L.; Rodríguez-Hornedo, N. Growth Kinetics and Mechanisms of Glycine Crystals. J. Cryst. Growth **1992**, *121*, 33–38.
88. Zipp, G.L.; Rodríguez-Hornedo, N. The Mechanism of Phenytoin Crystal-Growth. Int. J. Pharm. **1993**, *98*(1–3), 189–201.
89. Lechuga-Ballesteros, D.; Rodríguez-Hornedo, N. The Influence of Additives on the Growth Kinetics and Mechanism of L-Alanine Crystals. Int. J. Pharm. **1995**, *115*(2), 139–149.
90. Lechuga-Ballesteros, D.; Rodríguez-Hornedo, N. Effects of Molecular Structure and Growth Kinetics on the Morphology of L-Alanine Crystals. Int. J. Pharm. **1995**, *115*, 151–160.
91. Yip, C.M.; Ward, M.D. Atomic Force Microscopy of Insulin Single Crystals: Direct Visualization of Molecules and Crystal Growth. Biophys. J. **1996**, *71*(2), 1071–1078.
92. Malkin, A.J.; Kuznetsov, Y.G.; Glantz, W.; McPherson, A. Atomic Force Microscopy Studies of Surface Morphology and Growth Kinetics in Thaumatin Crystallization. J. Phys. Chem. **1996**, *100*(28), 11736–11743.
93. Yip, C.M.; Brader, M.L.; Defelippis, M.R.; Ward, M.D. Atomic Force Microscopy of Crystalline Insulins: The Influence of Sequence Variation on Crystallization and Interfacial Structure. Biophys. J. **1998**, *74*(5), 2199–2209.
94. Kuznetsov, Y.G.; Malkin, A.J.; McPherson, A. Atomic Force Microscopy Studies of Phase Separations in Macromolecular Systems. Phys. Rev. B: Condens. Matter **1998**, *58*(10), 6097–6103.
95. Volmer, M. Crystal Growth. Z. Physik. **1922**, *9*, 193.
96. Stranski, I.N. Zur Theorie Der Kristallwachstums. Z. Phys. Chem. **1928**, *136*, 259–278.
97. Burton, W.K.; Cabrera, N.; Frank, F.C. The Growth of Crystals and the Equilibrium Structure of Their Surfaces. Philosophical Transactions **1951**, A*243*, 299–358.
98. Chernov, A.A. Formation of Crystals in Solution. Contemporary Physics **1989**, *30*, 251–276.
99. Bennema, P. Spiral Growth and Surface Roughening: Development Since Burton, Cabrera and Frank. J. Cryst. Growth **1984**, *69*, 182–197.
100. Zipp, G.L.; Rodríguez-Hornedo, N. Phenytoin Crystal Growth Rates in the Presence of Phosphate and Chloride Ions. J. Cryst. Growth **1992**, *123*, 247–254.
101. Lechuga-Ballesteros, D.; Rodríguez-Hornedo, N. The Relation Between Absorption of Additives and Crystal Growth Rate of L-Alanine. J. Colloid Interface Sci. **1993**, *157*, 147–153.
102. Garside, J.; Janssen-Van Rosmalen, R.; Bennema, P. Verification of Crystal Growth Rate Equations. J. Cryst. Growth **1995**, *29*, 353–366.
103. Durbin, S.D.; Feher, G. Studies of Crystal Growth Mechanisms of Proteins by Electron Microscopy. J. Mol. Biol. **1990**, *212*(4), 763–774.
104. Sunagawa, I. *Morhology of Crystals*; Terra Scientific Publishing Company: Tokyo, Japan, 1987.
105. Himes, V.L.; Mighell, A.D.; De Camp, W.H. Structure of Carbamazepine: 5H-Dibenz[b,f]azepine-5-carboxamide. Acta Crystallogr. **1981**, B*37*, 2242–2245.
106. Behme, R.J.; Brooke, D. Heat of Fusion Measurement of a Low Melting Polymorph of Carbamazepine That Undergoes Multiple-phase Changes During Differential Scanning Calorimetry Analysis. J. Pharm. Sci. **1991**, *80*(10), 986–990.
107. McMahon, L.E.; Timmins, P.; Williams, A.; York, P. Characterization of Dihydrates Prepared from Carbamazepine Polymorphs. J. Pharm. Sci. **1996**, *85*(10), 1064–1069.
108. Krahn, F.U.; Mielck, J.B. Relations Between Several Polymorphic Forms and the Dihydrate of Carbamazepine. Pharm. Acta Helv. **1987**, *62*, 247–254.
109. Roberts, R.J.; Rowe, R.C. Influence of Polymorphism on the Young's Modulus and Yield Stress of Carbamazepine, Sulfathiazole, and Sulfanilamide. Int. J. Pharm. **1996**, *129*, 79–94.
110. Kaneniwa, N.; Ichikawa, J-I.; Yamaguchi, T.; Hayashi, K.; Watari, N.; Sumi, M. Dissolution Behavior of

Carbamazepine Polymorphs. Yakugaku Zasshi **1987**, *107*, 808–813.
111. Matsuda, Y.; Akazawa, R.; Teraoka, R.; Otsuka, M. Pharmaceutical Evaluation of Carbamazepine Modifications: Comparative Study for Photostability of Carbamazepine Polymorphs by Using Fourier-transformed Reflection-absorption Infrared Spectroscopy and Colorimetric Measurement. J. Pharm. Pharmacol. **1994**, *46*, 162–167.
112. Kobayasji, Y.; Ito, S.; Itai, S.; Yamamoto, K. Physicochemical Properties and Bioavailability of Carbamazepine Polymorphs and Dihydrate. Int. J. Pharm. **2000**, *193*, 137–146.
113. Lefebvre, C.; Guyot-Herman, A.M.; Draguet-Brughmans, M.; Bouche, R.; Guyot, J.C. Polymorphic Transitions of Carbamazepine During Grinding and Compression. Drug Dev. Ind. Pharm. **1986**, *12*, 1913–1927.
114. Lowes, M.M.; Caira, M.R.; Lotter, A.P.; Van Der Watt, J.G. Physicochemical Properties and X–ray Structural Studies of the Trigonal Polymorph of Carbamazepine. J. Pharm. Sci. **1987**, *76*(9), 744–752.
115. Ceoline, R.; Toscani, S.; Gardette, M.; Agafonov, V.N.; Dzyabchenko, A.V.; Bachet, B. X-ray Characterization of the Triclinic Polymorph of Carbamazepine. J. Pharm. Sci. **1997**, *86*(9), 1062–1065.
116. York, P. Solid-state Properties of Powders in the Formulation and Processing of Solid Dosage Forms. Int. J. Pharm. **1983**, *14*, 1–28.
117. Williams, R.O.; Brown, J.; Liu, J. Influence of Micronization Method on the Performance of a Suspension Triamcinolone Acetonide Pressurized Metered-Dose Inhaler Formulation. Pharm. Dev. Tech. **1999**, *4*(2), 167–179.
118. Chew, N.; Chan, H. Influence of Particle Size, Air, Flow, and Inhaler Device on the Dispersion of Mannitol Powders As Aerosols. Pharm. Res. **1999**, *16*(7), 1098–1103.
119. Vernaet, C.; Byron, P.R. Drug-Surfactant-Propellant Interactions in HFA-Formulations. Int. J. Pharm. **1999**, *186*(1), 13–30.
120. Sinclair, B.D.; Rodríguez-Hornedo, N. A Molecular Simulation Approach to Interpret the Effects of Intermolecular Interactions Between Additives and Crystal Surfaces on the Morphology of Carbamazepine Dihydrate, *In Preparation*.
121. Lechuga-Ballesteros, D.; Rodríguez-Hornedo, N. Growth and Morphology of D-Alanine Crystals: Influence of Additive Adsorption. Pharm. Res. **1993**, *10*, 1008–1014.
122. Berkovitch-Yellin, Z. Toward An Ab Initio Derivation of Crystal Morphology. J. Am. Chem. Soc. **1987**, *107*, 8239–8253.
123. Bravais, A. *Etudes Crystallographiques*; Gauthier-Villars: Paris, 1907.
124. Friedel, G. Bull. Soc. Fr. Mineral **1907**, *30*, 326–455.
125. Donnay, J.D.H.; Harker, D. A New Law of Crystal Morphology Extending the Law of Bravais. Am. Mineral. **1937**, *22*, 446–467.
126. Docherty, R.; Roberts, K.J. Modelling the Morphology of Molecular Crystals; Application to anthrancene, biphenyl, and β-succinic acid. J. Cryst. Growth **1988**, *88*, 159–168.
127. Clydesdale, G.; Docherty, R.; Roberts, K.J. HABIT — A Program for Predicting the Morphology of Molecular Crystals. Comput. Phys. Commun. **1991**, *64*, 311–328.
128. Hartman, P.; Perdok, W.G. On the Relations Between Structure and Morphology of Crystals. Acta Crystallographica **1955**, *8*, 49–52.
129. Hartman, P.; Bennema, P. The Attachment Energy As a Habit Controlling Factor. J. Cryst. Growth **1980**, *49*, 145–149.
130. Lifson, S.; Hagler, A.T.; Dauber, P. Consistent Force Field Studies of Intermolecular Forces in Hydrogen-bonded Crystals. J. Am. Chem. Soc. **1979**, *101*(18), 5111–5121.
131. Clydesdale, G.; Roberts, K.J.; Docherty, R. HABIT95 — A Program for Predicting the Morphology of Molecular Crystals As a Function of the Growth Environment. J. Cryst. Growth **1996**, *166*, 78–83.
132. Black, S.N.; Davey, R.J.; Halcrow, M. The Kinetics of Crystal–Growth in the Presence of Tailor–Made Additives. J. Cryst. Growth **1986**, *79*(1–3), 765–774.
133. Davey, R.J.; Black, S.N.; Goodwin, A.D.; Mackerron, D.; Maginn, S.J.; Miller, E.J. Crystallisation in Polymer Films: Control of Morphology and Kinetics of an Organic Dye in a Polysilicone Matrix. J. Mater. Chem. **1997**, *7*(2), 237–241.
134. Chen, B.D.; Garside, J.; Davey, R.J.; Maginn, S.J.; Matsuoka, M. Growth Of *M*–Chloronitrobenzene Crystals in the Presence of Tailor—Made Additives—Assignment of the Polar Axes from Morphological Calculations. J. Phys. Chem. **1994**, *98*(12), 3215–3221.
135. Etter, M.C. Hydrogen –Bonds As Design Elements in Organic Chemistry. J. Phys. Chem. **1991**, *95*(12), 4601–4610.
136. Rodríguez-Hornedo, N.; Murphy, D. Significance of Controlling Crystallization Mechanisms and Kinetics in Pharmaceutical Systems. J. Pharm. Sci. **1999**, *88*(7), 651–660.
137. Morris, K.; Rodríguez-Hornedo; Hydrates, N. *Encyclopedia of Pharmaceutical Technology*; Boylan, J.C., Swarbrick, J., Eds.; 1993; 393–440.
138. Nass, K.K. Process Implications of Polymorphism in Organic Compounds. AIChE **1991**, *284*, 72–81.

## FURTHER READING

Brittain, H.G. *Polymorphism in Pharmaceutical Solids*; Marcel Dekker, Inc.: New York, 1999.
Byrn, S.R.; Pfeiffer, R.R.; Stowell, J.G. *Solid-State Chemistry of Drugs*; SSCI, Inc.: West Lafayette, IN, 1999.
Chernov, A.A. *Modern Crystallography III: Crystal Growth*; Springer-Verlag: Berlin, 1980.
Cullity, B.D. *Elements of X-ray Diffraction*; Addison-Wesley Publishing Company, Inc.: Reading Massachusetts, 1978.
Gavezzotti, A. *Theoretical Apsects and Computer Modeling*; John Wiley & Sons Ltd.: New York, 1997.
Mersmann, A. *Crystallization Technology Handbook*; Marcel Dekker, Inc.: New York, 1995.
Mullin, J.W. *Crystallization*; Butterworth-Heinemann Ltd.: Oxford, 1993.
Myerson, A.S. *Handbook of Industrial Crystallization*; Butterworth-Heinemann Ltd.: Oxford, 1993.
Söhnel, O.; Garside, J. *Precipitation: Basic Principles and Industrial Applications*; Butterworth-Heinemann Ltd.: Oxford, 1992.
Zettlemoyer, A.C. *Nucleation*; Marcel Dekker, Inc.: New York, 1969.